molecules

MDPI

Article

# Mori Ramulus (Chin.Ph.)—the Dried Twigs of *Morus alba* L./Part 1: Discovery of Two Novel Coumarin Glycosides from the Anti-Hyperuricemic Ethanol Extract

**Jianbiao Yao [1], Houhong He [1], Jin Xue [1], Jianfang Wang [1], Huihui Jin [1], Jian Wu [1], Jiangning Hu [1], Ruwei Wang [1] and Kenny Kuchta [2,3,*]**

1 Zhejiang Provincial Key Laboratory of Traditional Chinese Medicine Pharmaceutical Technology, Hangzhou 310018, China; yaojb@conbagroup.com (J.Y.); hehh@conbagroup.com (H.H.); xuejin@conbagroup.com (J.X.); wangjf@conbagroup.com (J.W.); jinhh@conbagroup.com (H.J.); wujian@conbagroup.com (J.W.); hujn@conbagroup.com (J.H.) wangrw@conbagroup.com (R.W.)
2 Zhejiang Institute of TCM and Natural Medicine, Hangzhou 310018, China
3 Clinic for Gastroenterology and Gastrointestinal Oncology, University Medical Center Göttingen, Robert-Koch-Str. 40, 37075 Göttingen, Germany
* Correspondence: kenny.kuchta@med.uni-goettingen.de; Tel.: +49-(0)551-39-66391; Fax: +49-(0)551-39-9820

Academic Editor: Thomas Efferth
Received: 14 December 2018; Accepted: 12 January 2019; Published: 11 February 2019


**Abstract:** In Traditional Chinese Medicine (TCM), Mori ramulus (Chin.Ph.)—the dried twigs of *Morus alba* L.—is extensively used as an antirheumatic agent and also finds additional use in asthma therapy. As a pathological high xanthine oxidase (XO, EC 1.1.3.22) activity is strongly correlated to hyperuricemy and gout, standard anti-hyperuremic therapy typically involves XO inhibitors like allopurinol, which often cause adverse effects by inhibiting other enzymes involved in purine metabolism. Mori ramulus may therefore be a promissing source for the development of new antirheumatic therapeutics with less side effects. Coumarins, one of the dominant groups of bioactive constituents of *M. alba*, have been demonstrated to possess anti-inflammatory, antiplatelet aggregation, antitumor, and acetylcholinesterase (AChE) inhibitory activities. The combination of HPLC (DAD) and Q-TOF technique could give excellent separating and good structural characterization abilities which make it suitable to analyze complex multi-herbal extracts in TCM. The aim of this study was to develop a HPLC (DAD)/ESI-Q-TOF-MS/MS method for the identification and profiling of pharmacologically active coumarin glycosides in Mori ramulus refined extracts for used in TCM. This HPLC (DAD)/ESI-Q-TOF-MS/MS method provided a rapid and accurate method for identification of coumarin glycosides—including new natural products described here for the first time—in the crude extract of *M. alba* L. In the course of this project, two novel natural products moriramulosid A (umbelliferone-6-β-D-apiofuranosyl-(1→6)-β-D-glucopyranoside) and moriramulosid B (6-[[6-*O*-(6-deoxy-α-L-mannopyranosyl)-β-D-glucopyranosyl]oxy]-2*H*-1-benzopyran-1-one) were newly discovered and the known natural product Scopolin was identified in *M. alba* L. for the first time.

**Keywords:** *Morus alba* L.; coumarin glycosides; structural characterization; electrospray ionization; tandem mass spectrometry

## 1. Introduction

A pathological high xanthine oxidase (XO, EC 1.1.3.22) activity is strongly correlated to hyperuricemy and gout [1]. The prevalence of this disease is 2% to 9 % depending on age and gender and increases continuously in industrialized countries [2]. The pathological symptoms of gout emerge from the extracellular precipitation of monosodium urate crystals in different tissues (e.g., joints) followed by an inflammatory response [2,3]. An anti-hyperuremic therapy often includes the application of XO inhibitors like allopurinol. Upon reaction with the enzyme, allopurinol is oxidized to oxypurinol [2]. Whereas allopurinol is a weak competitive XO inhibitor, oxypurinol exhibits a strong non-competitive inhibitory effect [3]. Unfortunately, the use of the purine analog allopurinol in gout therapy shows adverse effects by inhibiting other enzymes involved in purine metabolism, making the search for alternative XO inhibitors necessary [2].

In this context, several ethnopharmacological approaches have been described [1,4], finding gallic and ellagic acids as well as several flavonoids as inhibitors of XO. Recently, testing of the pharmacological potential of Mediterranean plants by the consortium 'Local Food-Nutraceuticals' also included XO inhibitory studies [5]. For example, in Mediterranean traditional medicine olive leaf (*Olea europaea* L.) preparations such as aqueous decocts are used against gout and hypertension [6].

In Traditional Chinese Medicine, Mori ramulus (Chin.Ph.)—the dried twigs of *Morus alba* L.—are extensively used as an antirheumatic [7] agent. Just as several medical plants traditionally used for gout treatment (e.g., *Erythrina stricta* Roxb., *Cunonia macrophylla* Brongn. & Gris., *Olea europaea* L.) also exhibit antiinflammatory effects [6,8–12], the Mori ramulus drug also finds additional use in asthma therapy [13]. This fact as well as the structural complexity, specialized tissue distribution, and manifold regulatory mechanisms of XO strongly suggest a (patho-)physiological XO function beyond the purine metabolism [6].

Many potentially active constituents of *M. alba* such as flavonoids [14], benzofuran derivatives [15], stilbenes [16] and coumarins [17] have been identified in this herbal drug. Coumarins, one of these groups of bioactive constituents, have been demonstrated to possess anti-inflammatory [18], antiplatelet aggregation [19], antitumor [20], as well as both acetylcholinesterase (AChE) [21] and tyrosinase inhibitory activities [22]. Several methods have been reported for the analysis of natural products such as coumarin glycosides using LC-MS—including ion trap—and Q-TOF mass spectrometry [23]. The combination of HPLC (DAD) and Q-TOF technique could give excellent separating and good structural characterization abilities which make it suitable to analyze complex extracts in TCM [24–26]. The aim of this study was to develop a HPLC(DAD)/ESI-Q-TOF-MS/MS method for the identification and profiling of pharmacologically active coumarin glycosides in Mori ramulus refined extracts for used in TCM.

## 2. Results and Discussion

### *2.1. Structural Characterization and Fragmentation Behavior of Compounds **A** and **B** and **C***

The full-scan mass spectrum of the newly discovered natural product umbelliferone-6-β-D-apiofuranosyl-(1→6)-β-D-glucopyranoside (**A**) contains a $[M - H]^-$ ion at $m/z$ 455.1176, $[M + Cl - H]^-$ ion at $m/z$ 491.0944 and $[2M - H]^-$ ion at $m/z$ 911.2448 in the negative ESI source. The molecular formula of **A** was determined to be $C_{20}H_{24}O_{12}$ by HRESI-MS analysis [$m/z$ 455.1176 $(M - H)^-$]. In addition, a small abundant ion at $m/z$ 293.0842 was observed; this suggests Glc-Api residue was present in the structure. In MS/MS spectrum of this ion $[M - H]^-$, a product ion at $m/z$ 161.0235 was observed as a major product ion, resulting from the direct loss of Glc residue from $[M - Glc - Api]^-$. The ion at $m/z$ 161.0235 was very stable and did not yield any further fragmentation. We believe that the Glc residue elimination originate from C-7 of this ion. Consequently, the structure of the novel natural product **A** was identified as shown in Figure 1 (and Figure S1) and was named moriramulosid A.

A similar diagnostic fragmentation pattern was observed in the MS and MS/MS spectra of 6-[[6-*O*-(6-deoxy-α-L-mannopyranosyl)-β-D-glucopyranosyl]oxy]-2*H*-1-benzopyran-1-one (**B**). The UV

spectra were obtained for the two compounds. The results showed a local absorption maximum around 320 nm for both compounds in the UV spectrum data. Hence, it can be concluded that the fragmentation behavior and UV absorption of these analogue 6-substituent coumarin glycosides are indeed very similar. Consequently, the structure of the novel natural product **B** (Figure 2 and Figure S2) was identified as a second new natural product that was named moriramulosid B.

In the MS/MS spectrum of **A**, a product ion at $m/z$ 191 was observed, meanwhile, it is notably that fragment ion at $m/z$ 176 was labeled as [Y0 − 2H]−. The similar diagnostic fragmentation pattern was observed in the MS and MS/MS spectra of **C**; identified as Scopolin (Figure 3 and Figure S3). Its UV spectrum shows two local absorption maxima: one at ca. 285 nm (band II) and another at ca. 340 nm (band I).

### 2.1.1. Compound **A**

The $^{13}$C-NMR and DEPT spectra revealed that compound **A** contains a sugar chain. The $^{13}$C-NMR spectra of compound **A** displayed three sets characteristic for oxygen bearing methylene—$\delta_C$ 63.7 (C-6′), $\delta_C$ 73.5 (C-4″), $\delta_C$ 68.0 (C-5″)—seven methyne sets and one quaternary carbon atom (see Table 1). Combined with the $^1$H-NMR spectral data, it can be deduced that A contains one hexose group and one apiose group. For the aglycone part of A, the presence of two singlets at $\delta_H$ 6.34 (d, 9.5 Hz) and $\delta_H$ 8.00 (d, 9.5 Hz) in the $^1$H-NMR spectra and four singlets at $\delta_C$ 160.7, $\delta_C$ 155.4, $\delta_C$ 144.6, $\delta_C$ 113.8 in the $^{13}$C-NMR spectra, were in accord with substitution of benzopyranocoumarion. The presence of three aromatic protons at $\delta_H$ 7.04 (d, 2.2 Hz), $\delta_H$ 7.04 (dd, 9.3 Hz, 2.3 Hz), $\delta_H$ 7.66 (d, 9.3 Hz) assignable to the benzopyranocoumarion structural unit is a typical AMX coupled system, and clearly indicates a C-6 monosubstituted coumarin. The $^{13}$C-NMR signals of C-6 and C-6′, and $^1$H-NMR signals of H-1′ and H-1″ were assigned on the basis of HMBC connectivity observed for the sugar unit connecting with C-6 aglycone, which was shown by H-1′ and C-7, and H-1″ and C-6′, having long-distance correlations.

**Table 1.** $^1$H- and $^{13}$C-NMR Data for Compound **A**.

| No. | $^{13}$C | $^1$H |
|---|---|---|
| **Benzopyranocoumarion Structural Moiety** | | |
| 1 | 160.7 | / |
| 2 | 113.8 | 6.34 (1H, d, *J* = 9.5 Hz) |
| 3 | 144.6 | 8.00 (1H, d, *J* = 9.5 Hz) |
| 4 | 130.0 | 7.66 (1H, d, *J* = 9.3 Hz) |
| 5 | 113.8 | 7.04 (1H, d, *J* = 2.2 Hz) |
| 6 | 160.6 | / |
| 7 | 109.8 | 7.04 (1H, dd, *J* = 9.3 Hz, 2.3 Hz) |
| 8 | 155.4 | / |
| 9 | 113.8 | / |
| **Hexose Moiety** | | |
| 1′ | 100.4 | 5.02 (1H, d, *J* = 7.4 Hz) |
| 2′ | 76.8 | 3.45 (1H, d, *J* = 7.0 Hz) |
| 3′ | 73.8 | 3.46 (1H, d, *J* = 7.0 Hz) |
| 4′ | 70.3 | 3.13 (1H, t, *J* = 9.3 Hz) |
| 5′ | 76.0 | 3.26~3.29 (1H, m) |
| 6′ | 63.7 | 3.70~3.76 (2H, m) |
| **Apiose Moiety** | | |
| 1″ | 103.8 | 4.81 (1H, d, 3.1 Hz) |
| 2″ | 76.4 | 3.30~3.33 (1H, m) |
| 3″ | 79.2 | / |
| 4″ | 73.5 | 3.59~3.62 (2H, m) |
| 5″ | 68.0 | 3.87~3.91 (2H, m) |

### 2.1.2. Compound **B**

The NMR data of compound **B** are similar to those for compound **A**. **B** also contains a benzopyranocoumarion structural moiety: $\delta_H$ 6.35 (1H, d, 9.5 Hz), $\delta_H$ 8.01(1H, d, 9.5 Hz), $\delta_C$ 160.8, and a typical AMX coupled system: $\delta_H$ 7.66 (1H, d, 8.4 Hz), $\delta_H$ 7.03(1H, dd, 8.5 Hz, 2.4 Hz), $\delta_H$ 7.04 (1H, d, 2.4 Hz) (see Table 2). There are two hexose moieties in the sugar part, one of which contains a methyl group. The HMBC cross-peaks of H-1′ with C-7 and H-1″ with C-6′ indicated that the sugar unit is connected with C-6 aglycone.

**Table 2.** $^1$H- and $^{13}$C-NMR Data for Compound **B**.

| No. | $^1$H-NMR | $^{13}$C-NMR |
|---|---|---|
| **Benzopyranocoumarion Structural Moiety** | | |
| 1 | / | 160.8 |
| 2 | 6.35 (1H, d, *J* = 9.5 Hz) | 113.8 |
| 3 | 8.01 (1H, d, *J* = 9.5 Hz) | 144.7 |
| 4 | 7.66 (1H, d, *J* = 8.4 Hz) | 113.8 |
| 5 | 7.03 (1H, dd, *J* = 8.5 Hz, 2.4 Hz) | 103.9 |
| 6 | / | 160.6 |
| 7 | 7.04 (1H, d, *J* = 2.4 Hz) | 101.0 |
| 8 | / | 155.4 |
| 9 | / | 113.6 |
| **Hexose moiety** | | |
| 1′ | 5.03 (1H, d, *J* = 7.4 Hz) | 100.5 |
| 2′ | 3.51 (1H, d, *J* = 3.4 Hz) | 76.9 |
| 3′ | 3.50 (1H, d, *J* = 3.2 Hz) | 73.5 |
| 4′ | 3.14~3.16 (1H, m) | 70.2 |
| 5′ | 3.26~3.29 (1H, m) | 76.0 |
| 6′ | 3.82~3.94 (2H, m) | 66.6 |
| 1″ | 4.53 (1H, d, *J* = 1.3 Hz) | 101.0 |
| 2″ | 3.45~3.49 (1H, m) | 72.3 |
| 3″ | 3.41~3.44 (1H, m) | 70.8 |
| 4″ | 3.17~3.20 (1H, m) | 68.8 |
| 5″ | 3.30~3.32 (1H, m) | 71.1 |
| 6″-Me | 1.08 (3H, d, *J* = 6.3 Hz) | 68.2 |

### 2.1.3. Compound **C**

The $^{13}$C-NMR and DEPT spectra revealed that compound **C** contains a monosaccharide, and the glycosyl group has six carbon signals. The $^{13}$C-NMR spectra of compound **C** displayed one oxygen bearing a methylene characteristic set—$\delta_C$ 61.1 (6′-C)—and five methyne sets. Combined with the $^1$H-NMR spectral data, it can be concluded that C contains one glucose group. For the aglycone part of C, the presence of two singlets at $\delta_H$ 6.33 (1H, d, 9.5 Hz) and $\delta_H$ 7.97 (1H, d, 9.5 Hz) in the $^1$H-NMR spectra and one carbonyl carbon singlet at $\delta_C$ 160.7 in the $^{13}$C-NMR spectra, are in accordance with substitution of benzopyranocoumarion. The presence of singlets of a methoxy group at $\delta_H$ 3.83 and of an aromatic single hydrogen at $\delta_H$ 7.30, $\delta_H$ 7.16 in the $^1$H-NMR spectra, demonstrates that C-5 and C-6 of the benzopyranocoumarion are substituted (see Table 3).

Based on these data, compound **C** was identified as Scopolin, a previously known natural product that was identified as a constituent of *Morus alba* L. for the first time in the present study.

**Table 3.** $^{1}$H- and $^{13}$C-NMR Data for Compound **C**.

| No. | $^{1}$H-NMR | $^{13}$C-NMR |
|---|---|---|
| **Benzopyranocoumarion Structural Moiety** | | |
| 1 | / | 160.9 |
| 2 | 6.33 (1H, d, *J* = 9.5 Hz) | 110.2 |
| 3 | 7.97 (1H, d, *J* = 9.5 Hz) | 144.6 |
| 4 | 7.30 (1H, s) | 113.7 |
| 5 | / | 149.4 |
| 6 | / | 150.4 |
| 7 | 7.16 (1H,s) | 103.5 |
| 8 | / | 146.5 |
| 9 | / | 112.7 |
| 10-OMe | 3.83 (3H, s) | 56.5 |
| **Hexose Moiety** | | |
| 1′ | 5.09 (1H, d, *J* = 7.4 Hz) | 100.2 |
| 2′ | 3.40~3.44 (1H, m) | 73.5 |
| 3′ | 3.30~3.33 (1H, m) | 77.2 |
| 4′ | 3.17 (1H, t, *J* = 9.0 Hz) | 70.1 |
| 5′ | 3.28~3.30 (1H, m) | 77.6 |
| 6′ | 3.45~3.48 (1H, m)<br>3.68~3.71 (1H, m) | 61.1 |

**a**

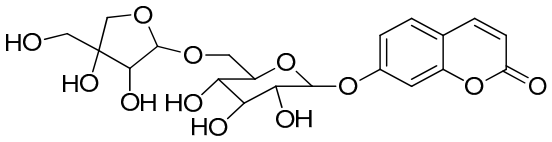


**b**

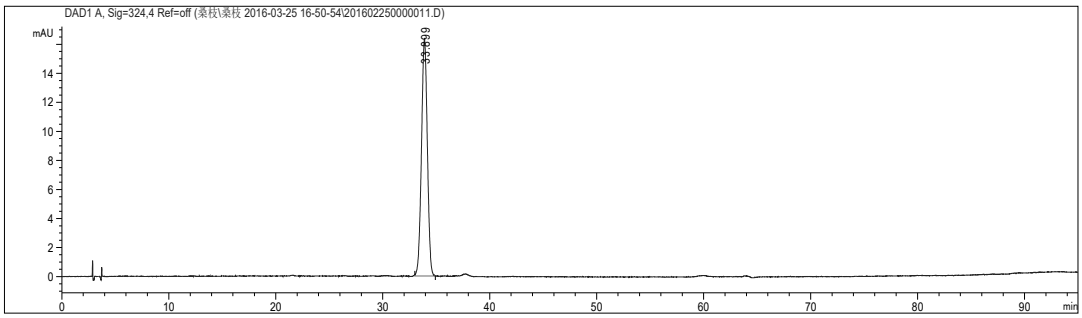


**Figure 1.** (**a**) Structure of compound **A** $C_{20}H_{24}O_{12}$, moriramulosid A (umbelliferone-6-β-D-apiofuranosyl-(1→6)-β-D-glucopyranoside); (**b**) HPLC chromatogram of moriramulosid A (umbelliferone-6-β-D-apiofuranosyl-(1→6)-β-D-glucopyranoside). Details of the HPLC-MS method, see main text.

**a**

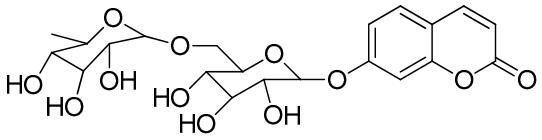

**b**

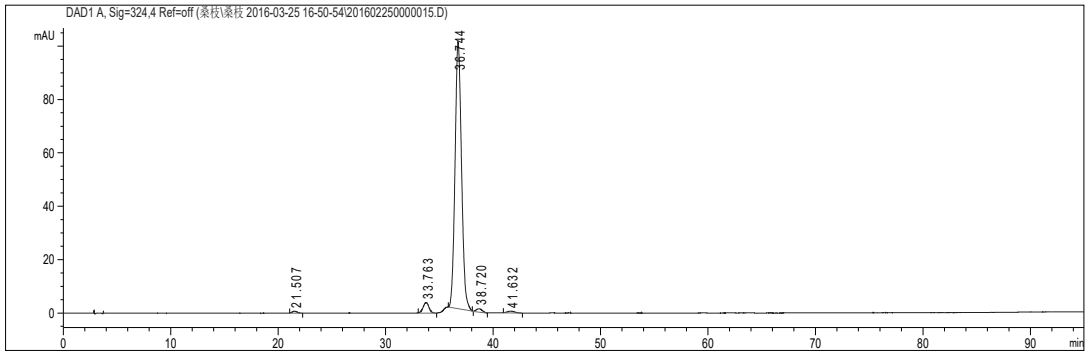


**Figure 2.** (**a**) Structure of compound **B** $C_{21}H_{26}O_{12}$, moriramulosid B (6-[[6-*O*-(6-deoxy-α-L-mannopyranosyl)-β-D-glucopyranosyl]oxy]-2*H*-1-benzopyran-1-one); (**b**) HPLC chromatogram of moriramulosid B (6-[[6-*O*-(6-deoxy-α-L-mannopyranosyl)-β-D-glucopyranosyl]oxy]-2*H*-1-benzopyran-1-one). Details of the HPLC-MS method, see main text.

**a**

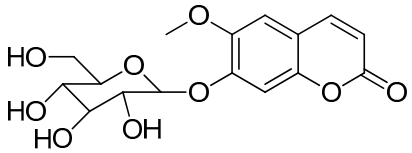

**b**

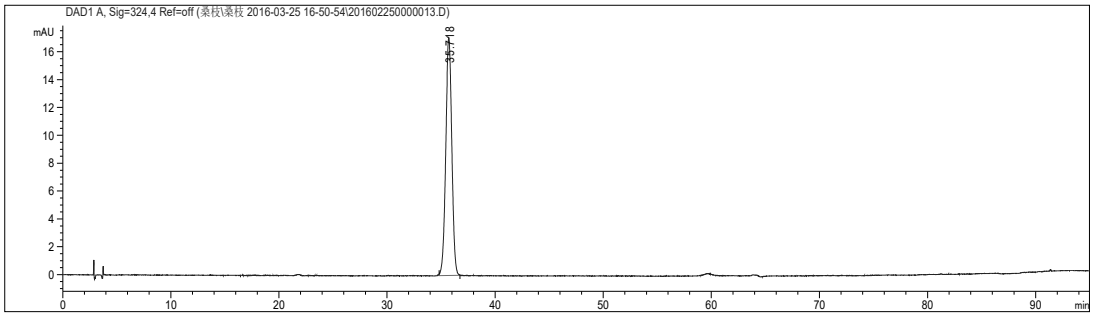


**Figure 3.** (**a**) Structural formula of compound **C** $C_{16}H_{18}O_9$, Scopolin; (**b**) HPLC chromatogram of Scopolin. Details of the HPLC-MS method, see main text.

## 2.2. Anti-Hyperuricemic Activity In Vivo

In order to study the effect of the Mori ramulus refined extract ZY1402-A on the serum uric acid levels, in vivo experiments in a mouse model were performed. Therefore, 32 adult male SPF Kunming mice (body weight each between 18 and 22 g) were randomly divided into four groups ($n$ = 8), namely the healthy control group (C), the placebo model group (M), the allopurinol positive control group (A), and the group treated with the Mori ramulus refined extract ZY1402-A. All mice were treated by intragastric administration (ig) daily (at 9:00 am) for 8 days. All groups with the exception of the healthy control group (C) were treated (ig) with 300 mg/kg potassium oxonate 1 h before the respective treatment was administered. Blood was collected from the posterior venous plexus of the eye after 1 h of administration of the respective treatment on the 8th day. Subsequently, serum was taken after centrifugation for measuring the levels of serum uric acid ($S_{UA}$). For further details see Section 4.5.

Compared with the healthy control group the serum uric acid levels of the placebo model group were significantly increased. Compared with the placebo model group, both the serum uric acid levels

of the positive control group (5 mg/kg allopurinol) and the Mori ramulus refined extract (ZY1402-A) treatment group and were significantly reduced (Figure 4).

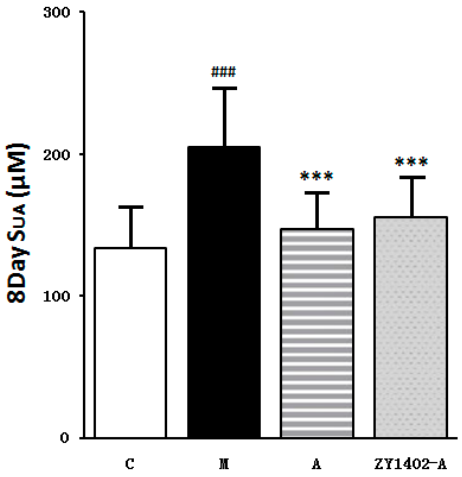


**Figure 4.** The effect of the Mori ramulus refined extract ZY1402-A on serum uric acid levels in the in vivo mouse model ($n$ = 8; ### $p < 0.001$ compared to C; *** $p < 0.001$ compared to M). All data are given as X ± SD. Healthy control group (C), placebo model group (M), allopurinol positive control group (A).

## 3. Conclusions

In the present study, two novel natural products from the class of coumarin glycosides—moriramulosid A and B—were isolated and identified for the first time from an ethanol extract of Mori ramulus (Chin.Ph.). Said extract was characterized using negative ion HPLC/ESI-Q-TOF-MS/MS spectra in combination to UV-DAD. This HPLC/ESI-Q-TOF-MS/MS method provided a rapid and accurate method for identification of coumarin glycosides in crude extract from *M. alba* L.

The accompanying mouse model experiments for measuring the anti-hyperuricemic activity of the Mori ramulus refined extract (ZY1402-A) in vivo demonstrate that this extract can reduce the serum uric acid levels of SPF Kunming mice significantly.

## 4. Experimental

### *4.1. Extract Preparation, Reagents, and Chemicals*

Mori ramulus (Chin.Ph.)—the dried twigs of *Morus alba* L.—(batch No. 20150113-2) were purchased via Chuxiongtengyang Chinese Herbal Medicine Corporation, from Good Agricultural Practice (GAP) cultivation sites (Figure 5) in Yunnan, China. The plant material was taxonomically identified by the author Houhong He and a voucher specimen (accession No. 20150113) was deposited at the herbarium of Zhejiang CONBA Pharmaceutical, China.

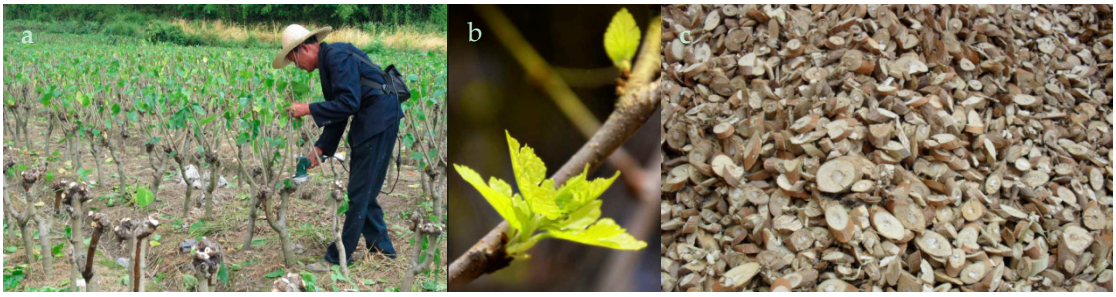


**Figure 5.** Photos taken at a GAP cultivation site for *Morus alba* L. in Yunnan, China. (**a**) Farmer harvesting *Morus alba* twigs; (**b**) Young leaved sprouting on the *Morus alba* twigs in spring; (**c**) Mori ramulus drug in market form. Although more than 10,000,000 tons of mulberry twigs are produces in the Peoples Republic of China annually, only a small percentage is used as medicine, whereas most is treated as agricultural waste or as firewood.

1002.8 g of dried and powdered Mori ramulus (Chin.Ph.) drug were soaked with 60% ethanol (Carl Roth, Karlsruhe, Germany) overnight, and subsequently extracted twice with 7.0 L of 60% ethanol under reflux for 2 h each. After filtration, the liquid extract was evaporated to dryness under reduced pressure resulting in 5.127 g of dry extract residue, which was subsequently dissolved in 90% ethanol. This ethanol solution was precipitated by adding water in order to obtain the aqueous solution of its water soluble constituents. These were subsequently adsorbed to HPD-100 macroporous resin (Cangzhou Bao'en Adsorbing Material Technology, Cangzhou, China), which was eluted with 25% ethanol. Finally, this eluent was evaporated to dryness under reduced pressure, thus yielding the final Mori ramulus (Chin.Ph.) refined extract that was named ZY1402-A.

HPLC grade acetonitrile, methanol, and analytical grade $CH_3COOH$ were utilized for HPLC analysis. Three compounds **A**, **B**, and **C** were isolated and purified from the above described refined extract of Mori ramulus (Chin.Ph.). Their structures were determined by the analysis of UV, NMR, MS spectra and compared with previous literature. The purities of isolates were over 95%, determined by HPLC/DAD analysis based on a peak area normalization method. The standard solution of each compound was prepared by dissolving it in 60% ($v/v$) methanol and stored at 4 °C until analysis.

### *4.2. Chromatography*

HPLC was performed on an Agilent series 1260 instrument (Agilent, Waldbronn, Germany) equipped with a quaternary pump, a diode-array detector (DAD), an autosampler, and a column compartment. The sample was separated on an Xtimate XB-C18 column (5 µm, 4.6 × 250 mm, Welch Materials, Shanghai, China). The mobile phase consisted of acetonitrile (mobile phase A); water ($H_2O$) containing 0.2% ($v/v$) $CH_3COOH$ (mobile phase B); and 5% ($v/v$) $CH_3OH$ (mobile phase C). The flow rate was 1 mL/min, and column temperature was set at 25 °C. The development of the gradient over time is summarized in Table 4. The DAD detector was monitored at 324 nm, and the on line UV spectra were recorded in the range 190–400 nm.

**Table 4.** HPLC gradient.

| Time (min) | Mobile Phase A (%) | Mobile Phase B (%) | Mobile Phase C (%) |
|---|---|---|---|
| 0~50 | 4 | 5 | 91 |
| 50~60 | 4→6 | 5 | 91→89 |
| 60~60.01 | 6→5 | 5→6 | 89 |
| 60.01~70 | 5→7 | 6 | 89→87 |
| 70~80 | 7→12 | 6 | 87→82 |
| 80~85 | 12→17 | 6 | 82→77 |
| 85~90 | 17→0 | 6→100 | 77→0 |
| 90~95 | 0 | 100 | 0 |

### *4.3. Mass Spectrometry*

An Aglient 6530 Q-TOF mass spectrometer (Agilent, Santa Clara, CA, USA) was connected to the Agilent 1260 HPLC instrument via an ESI interface. The acquisition parameters were as follows: drying gas ($N_2$) flow rate, 12.0 L/min; temperature, 350 °C; nebulizer, 60 psig; capillary, 4500 V; fragmentor, 175 V; skimmer, 65 V; OCT RF V, 750 V. Each sample was analyzed in both positive and negative ion mode to provide complimentary information for molecular formulae and structural identification. The quasi-molecular ion $[M - H]^-$ of interest in the negative ESI mode MS scan was selected as precursor ion and subjected to Target-MS/MS or Auto-MS/MS analyses. The collision energy (CE) was set at 35 V and the mass range recorded $m/z$ 100–2000.

### *4.4. NMR Spectroscopy*

NMR spectra were recorded in deuterated dimethyl sulfoxides (DMSO-d6) or methanol (MeOD) on a Bruker DRX-500 spectrometer (Bruker biospin, Rheinstetten, Germany) operating at 500 MHz for $^1H$ and at 125 MHz for $^{13}C$ including Distortionless Enhancement by Polarization Transfer (DEPT-135) measurements. Chemical shifts are persented in ppm downfield of tetramethylsilane. 1D and 2D NMR experiments were recorded using Mest NOVA software (Mestrelab Research, Santiago de Compostela, Spain).

### *4.5. Anti-Hyperuricemic Activity*

In order to study the effect of the Mori ramulus refined extract ZY1402-A on the serum uric acid levels, in vivo experiments in a mouse model were performed based on the mouse model developed by Wang M. et al. 2016 [27]. Therefore, 32 adult male SPF Kunming mice (body weight each between 18 and 22 g) obtained from the Shanghai Jiesijie Experiment Animal (Shanghai, China) were acclimatized for two days under 12 h/day light cycle (environment temperature 25 ± 2 °C) and food and drinking water ad libitum. Mice were randomly divided into four groups ($n$ = 8), namely the healthy control group (C), the placebo model group (M), the allopurinol positive control group (A), and the group treated with the Mori ramulus refined extract ZY1402-A. All mice were treated by intragastric administration (ig) daily (at 9:00 am) for 8 days. All groups with the exception of the healthy control group (C) were treated (ig) with 300 mg/kg potassium oxonate 1 h before the respective treatment was administered. Blood was collected from the posterior venous plexus of the eye in mice after 1 h of administration in the eighth day, and serum was taken after centrifugation. The levels of serum uric acid ($S_{UA}$) were measured. All data were expressed by X ± SD. SPSS19.0 one-way analysis of variance (ANOVA) was used to look at the statistical difference between the groups.

All animal maintenance and experimental studies were based on the guidelines of the National Institutes of Health for the Care and Use of Animals of the People's Republic of China, and were approved by the Experiment Animal Center of Nanjing University.

**Supplementary Materials:** The following are available online at http://www.mdpi.com/1420-3049/24/3/629/s1. Figures S1–S3.

**Author Contributions:** Conceptualization, R.W. and K.K.; methodology, J.Y., H.H., and R.W.; software, J.W. (Jian Wu), and J.H.; validation, J.W. (Jianfang Wang), H.J., J.W. (Jian Wu), and J.H.; formal analysis, J.W. (Jian Wu), and J.H.; investigation, J.Y., H.H., J.X., J.W. (Jianfang Wang), H.J., J.W. (Jian Wu), and J.H.; resources, R.W.; data curation, J.W. (Jian Wu); writing—original draft preparation, J.Y. and H.H.; writing—review and editing, K.K.; visualization, J.W. (Jianfang Wang); supervision, R.W. and K.K.; project administration, R.W. and K.K.

**Funding:** This research received no external funding.

**Acknowledgments:** Hans Rausch of Phytochem Referenzsubstanzen, Ichenhausen (Germany), is kindly acknowledged for his support and helpful consultation, especially concerning the interpretation of NMR data.

**Conflicts of Interest:** The authors declare no conflict of interest.

## References


1. Cos, P.; Ying, L.; Calomme, M.; Hu, J.P.; Cimanga, K.; Van, P.B.; Pieters, L.; Vlietinck, A.J.; Vanden, B.D. Structure-activity relationship and classification of flavonoids as inhibitors of xanthine oxidase and superoxide scavengers. *J. Nat. Prod.* **1998**, *61*, 71–76. [CrossRef] [PubMed]
2. Pacher, P.; Nivorozhkin, A.; Szabo, C. Therapeutic effects of xanthine oxidase inhibitors: Renaissance half a century after the discovery of allopurinol. *Pharmacol. Rev.* **2006**, *58*, 87–114. [CrossRef] [PubMed]
3. Mittal, A.; Phillips, A.R.; Loveday, B.; Windsor, J.A. The potential role for xanthine oxidase inhibition in major intra-abdominal surgery. *World J. Surg.* **2008**, *32*, 288–295. [CrossRef] [PubMed]
4. Lespade, L.; Bercion, S. Theoretical study of the mechanism of inhibition of xanthine oxidase by flavonoids and gallic acid derivatives. *J. Phys. Chem. B* **2010**, *114*, 921–928. [CrossRef] [PubMed]
5. Heinrich, M.; Müller, W.E.; Galli, C. *Local Mediterranean Food Plants and Nutraceuticals*; Forum of Nutrition; Karger: Basel, Switzerland, 2006; Volume 59, pp. 1–17, ISBN 978-3-8055-8124-0.
6. Flemmig, J.; Kuchta, K.; Arnhold, J.; Rauwald, H.W. Olea europaea leaf (Ph.Eur.) extract as well as several of its isolated phenolics inhibit the gout-related enzyme xanthine oxidase. *Phytomedicine* **2011**, *18*, 561–566. [CrossRef] [PubMed]
7. Seo, C.S.; Lim, H.S.; Jeong, S.J.; Ha, H.; Shin, H.K. HPLC-PDA analysis and anti-inflammatory effects of Mori Cortex Radicis. *Nat. Prod. Commun.* **2013**, *8*, 1443–1446. [PubMed]
8. Cecchini, T. *Enciclopedia de las Hierbas Medicinales*; Olivio: Barcelona, Spain, 1992; pp. 373–374, ISBN 84-315-1064-1.
9. Fogliani, B.; Raharivelomanana, P.; Bianchini, J.P.; Bouraima-Madjebi, S.; Hnawia, E. Bioactive ellagitannins from Cunonia macrophylla, an endemic Cunoniaceae from New Caledonia. *Phytochemistry* **2005**, *66*, 241–247. [CrossRef] [PubMed]
10. Leporatti, M.L.; Posocco, E.; Pavesi, A. Some new therapeutic uses of several medicinal plants in the province of Terni (Umbria, Central Italy). *J. Ethnopharmacol.* **1985**, *14*, 65–68. [CrossRef]
11. Scheffler, A.; Rauwald, H.W.; Kampa, B.; Mann, U.; Mohr, F.W.; Dhein, S. Olea europaea leaf extract exerts L-type Ca(2+) channel antagonistic effects. *J. Ethnopharmacol.* **2008**, *120*, 233–240. [CrossRef]
12. Umamaheswari, M.; Asokkumar, K.; Sivashanmugam, A.T.; Remyaraju, A.; Subhadradevi, V.; Ravi, T.K. In vitro xanthine oxidase inhibitory activity of the fractions of Erythrina stricta Roxb. *J. Ethnopharmacol.* **2009**, *124*, 646–648. [CrossRef]
13. Kim, H.J.; Lee, H.J.; Jeong, S.J.; Lee, H.J.; Kim, S.H.; Park, E.J. Cortex Mori Radicis extract exerts antiasthmatic effects via enhancement of CD4(+)CD25(+)Foxp3(+) regulatory T cells and inhibition of Th2 cytokines in a mouse asthma model. *J. Ethnopharmacol.* **2011**, *138*, 40–46. [CrossRef] [PubMed]
14. Wan, L.Z.; Ma, B.; Zhang, Y.Q. Preparation of morusin from Ramulus mori and its effects on mice with transplanted H22 hepatocarcinoma. *Biofactors* **2014**, *40*, 636–645. [CrossRef] [PubMed]
15. Dat, N.T.; Jin, X.; Lee, K.; Hong, Y.S.; Kim, Y.H.; Lee, J.J. Hypoxia-inducible factor-1 inhibitory benzofurans and chalcone-derived diels-alder adducts from Morus species. *J. Nat. Prod.* **2009**, *72*, 39–43. [CrossRef] [PubMed]
16. Zhang, Z.; Shi, L. Anti-inflammatory and analgesic properties of cis-mulberroside A from Ramulus mori. *Fitoterapia* **2010**, *81*, 214–218. [CrossRef] [PubMed]
17. Oh, H.; Ko, E.K.; Jun, J.Y.; Oh, M.H.; Park, S.U.; Kang, K.H.; Lee, H.S.; Kim, Y.C. Hepatoprotective and free radical scavenging activities of prenylflavonoids, coumarin, and stilbene from Morus alba. *Planta Med.* **2002**, *68*, 932–934. [CrossRef] [PubMed]
18. Wang, M.; Zhao, J.; Zhao, Y.; Huang, R.Y.; Li, G.; Zeng, X.; Li, X. A new coumarin isolated from Sarcandra glabra as potential anti-inflammatory agent. *Nat. Prod. Res.* **2016**, *30*, 1796. [CrossRef] [PubMed]
19. Kontogiorgis, C.; Nicolotti, O.; Mangiatordi, G.F.; Tognolini, M.; Karalaki, F.; Giorgio, C.; Patsilinakos, A.; Carotti, A.; Hadjipavlou-Litina, D.; Barocelli, E. Studies on the antiplatelet and antithrombotic profile of anti-inflammatory coumarin derivatives. *J. Enzyme Inhib. Med. Chem.* **2015**, *30*, 925–933. [CrossRef] [PubMed]
20. Liu, M.M.; Chen, X.Y.; Huang, Y.Q.; Feng, P.; Guo, Y.L.; Yang, G.; Chen, Y. Hybrids of phenylsulfonylfuroxan and coumarin as potent antitumor agents. *J. Med. Chem.* **2014**, *57*, 9343–9356. [CrossRef]
21. Fallarero, A.; Oinonen, P.; Gupta, S.; Blom, P.; Galkin, A.; Mohan, C.G.; Vuorela, P.M. Inhibition of acetylcholinesterase by coumarins: The case of coumarin 106. *Pharmacol. Res.* **2008**, *58*, 215–221. [CrossRef]

22. Zhang, L.; Tao, G.; Chen, J.; Zheng, Z.P. Characterization of a New Flavone and Tyrosinase Inhibition Constituents from the Twigs of *Morus alba* L. *Molecules* **2016**, *21*, 1130. [CrossRef]
23. Krieger, S.; Hayen, H.; Schmitz, O.J. Quantification of coumarin in cinnamon and woodruff beverages using DIP-APCI-MS and LC-MS. *Anal. Bioanal. Chem.* **2013**, *405*, 8337–8345. [CrossRef] [PubMed]
24. Locatelli, M. Anthraquinones: Analytical techniques as a novel tool to investigate on the triggering of biological targets. *Curr. Drug Targets* **2011**, *12*, 366–380. [CrossRef] [PubMed]
25. Locatelli, M.; Melucci, D.; Carlucci, G.; Locatelli, C. Recent HPLC strategies to improve sensitivity and selectivity for the analsis of complex matrices. *Instrum. Sci. Technol.* **2012**, *40*, 112–137. [CrossRef]
26. Zaza, S.; Lucini, S.M.; Sciascia, F.; Ferrone, V.; Cifelli, R.; Carlucci, G.; Locatelli, M. Recent Advances in the Separation and Determination of Impurities in Pharmaceutical Products. *Instrum. Sci. Technol.* **2015**, *43*, 182–196. [CrossRef]
27. Wang, M.; Zhao, J.; Zhang, N.; Chen, J. Astilbin improves potassium oxonate-induced hyperuricemia and kidney injury through regulating oxidative stress and inflammation response in mice. *Biomed. Pharmacother.* **2016**, *83*, 975–988. [CrossRef] [PubMed]